# Chapter 4

# POP online particle tracking of the Leeuwin Current System

## 4.1 INTRODUCTION

The aim of this chapter is to establish links between the large scale ocean circulation and the Leeuwin Current and the Leeuwin Undercurrent using an online particle tracking performed during the POP11B integration [model details in **Appendix C**]. We believe this will give insight into how and from where the Leeuwin Current waters originate, and where they spread after passing through the system. Inferences from water mass analyses for the Leeuwin Current are limited due to vigorous air–sea interactions along the path of the current.

## 4.2 PARTICLE TRACKING AND SELECTION CRITERIA

The Lagrangian diagnostics were obtained from a particle tracking calculation performed by Matthew Maltrud during the 5–year integration of POP11B (1993/97) and comprise time series of salinity (S), potential temperature ($\theta$), velocity (u,v,w), depth, latitude and longitude for each numerical particle. Particles were released every 20 days at chosen grid points, which collectively resemble the proposed WOCE lines [**Figure 4.1**], and at different start depths (75, 150, 300, 600, 900 and 1200 m). Start depths were also placed at 25 m in certain locations of the Indonesian Throughflow (Java, Halmahera, Molucca Seas and Makassar Strait) and Torres Strait, among others. The limited release in location and in frequency were designed to avoid computational overheads. Despite the fact that the total number of particles released in the online tracking is not large enough to conduct a quantitative study, the experiment provides insight on links between current regimes that are often difficult to understand in Eulerian diagnostics.

The displacements of the numerical particles were computed at each model time step ($\Delta t$ = 30 min) using a predictor–corrector scheme, and then saved into files as daily averages [Maltrud *et al.* 1998]. The predictor–corrector method is a numerical iteration

consisting of a guess for the prediction equation based on the Euler approximation and a correction equation using the trapezoidal rule. Although the time–stepping was formally of first order, but originally thought of second order, tests conducted in the open ocean against a fourth order time–stepping showed no statistical difference between the two approaches [Maltrud, *pers. comm.*]. The tracking procedure relies entirely on the three dimensional velocity field and does not take into account any implied (vertical, in particular) motion parameterised as mixing. This appears relevant just where vertical mixing plays a significant role in water motion, such as in deep convection sites. A typical problem of numerical particle trackings, known as "beached" particles, occurs when displacements are trapped incorrectly due to errors in the spatial interpolation and time extrapolation in grid cells that include a landmass point where a zero velocity is imposed [Garraffo *et al.*, 2001a; Garraffo *et al.*, 2001b]. This usually happens when particles lie within half grid cells over topography. As this problem cannot be avoided, "beached" particles are simply discarded.
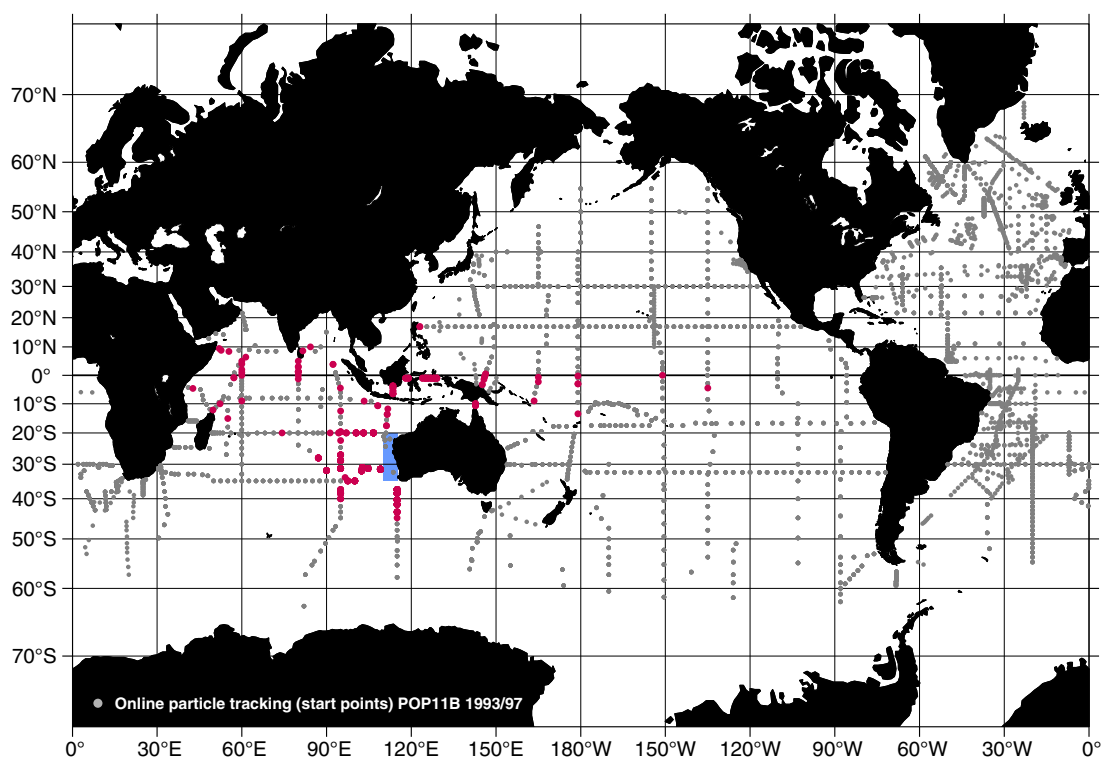


**Figure 4.1.** Global POP11B Lagrangian grid (gray and red circles). The shaded (blue) area denotes the selection area off Western Australia used as a criterion to separate the numerical particles for this study and the red circles are their associated start points.

To set apart the circulation associated with the Leeuwin Current and Leeuwin Undercurrent from the global Lagrangian grid, we only examine the trajectories which intersected an ocean region off Western Australia, from 20°S to 35°S and from 110°E to 115°E [see blue area in **Figure 4.1**]. After this, we discarded those particles that had start points inside the area in question as well as any particle whose start point was situated in depths greater than 600 m (particles with start points at 900 and 1200 m did not move far away from their release points over the 5–year simulation). We also removed "beached" particles, or whenever possible, blanked their time series from the instant they got "beached". The 574 particle trajectories used in this study [their start points are highlighted by red circles in **Figure 4.1**] were further divided in groups according to the distribution of start points and pathways to help visualise the various current regimes under investigation [**Tables 4.1** and **4.2**].

## 4.3    TRAJECTORIES

The trajectories of the water particles selected for this study traverse the Leeuwin Current, the Leeuwin Undercurrent, the Eastern Gyral Current and zonal flows in the southeastern Indian Subtropical Gyre [**Figure 4.2**]. The salinity changes, evidenced by the coloured trajectories, are an indicator of the diverse environments through which the water particles traverse.

The particles which traverse the Leeuwin Current originate from remote areas as far as the western/central tropical Pacific and the Somali Basin in the tropical Indian Ocean [panel a]. In both oceans, near equatorial surface currents (upper 100 m) advect particles towards the Indonesian Archipelago which then reach the Indo–Australian Basin via the South Java Current (Indian) and the Indonesian Throughflow (Pacific). Once in the Indo–Australian Basin, these particles subsequently travel along and across the westward–flowing South Equatorial Current (~10°–15°S) and eastward–flowing Eastern Gyral Current (~16°–20°S) before joining the poleward Leeuwin Current along the Australian coast. Start points associated with near surface eastward flows in the Subtropical Gyre also augment the Leeuwin Current, though the bulk of these eastward moving particles join the Leeuwin Undercurrent [panel b].

In addition to highly saline Subtropical Water, the Leeuwin Undercurrent receives relatively fresher and cooler South Indian Central Water from near the Subtropical Front (~40°–45°S) [Stramma, 1992; Belkin and Gordon, 1996; Stramma and Lutjeharms, 1997]. Most of the particles advected equatorward by the Leeuwin Undercurrent leave the coast to feed into a westward flow off Western Australia whereas a small number escapes to the Indo–Australian Basin. There, together with particles of the Eastern Gyral Current which had not joined the Leeuwin Current, they form an anticlockwise gyre. None of them are seen to cross the straits into the Indonesian Seas but they suggest a

southern source for part of the South Equatorial Current. The overall circulation pattern described above is represented by the schematic diagram in **Figure 4.3**.

**Table 4.1.** Distribution of the particle trajectories in start groups, start depths and pathways. Contribution to the Leeuwin Current.

| Group | Tropical Pacific | | Indonesian Throughflow | | Tropical Indian | | Eastern Gyral | Subtropical Indian |
|---|---|---|---|---|---|---|---|---|
| Route | S | C | S | C | S | C | | |
| 25 m | - - - | - - - | 24 | 18 | - - - | - - - | - - - | - - - |
| 75 m | 10 | 8 | 5 | 9 | 10 | 25 | 19 | 13 |
| 150 m | ∅ | ∅ | 1 | ∅ | ∅ | 2 | ∅ | ∅ |
| 300 m | ∅ | ∅ | ∅* | ∅* | ∅ | 1 | ∅ | ∅ |
| 600 m | ∅ | ∅ | ∅* | ∅* | ∅ | ∅ | ∅ | ∅ |
| Sum | 10 | 8 | 30 | 27 | 10 | 28 | 19 | 13 |
| Total | 18 + 57 + 38 + 19 = **132** | | | | | | | 13 |

- - -  No Coverage          * Location shallower than the depth level

**Table 4.2.** Distribution of the particle trajectories in start groups and start depths. Contribution to the Leeuwin Undercurrent and Subtropical Gyre.

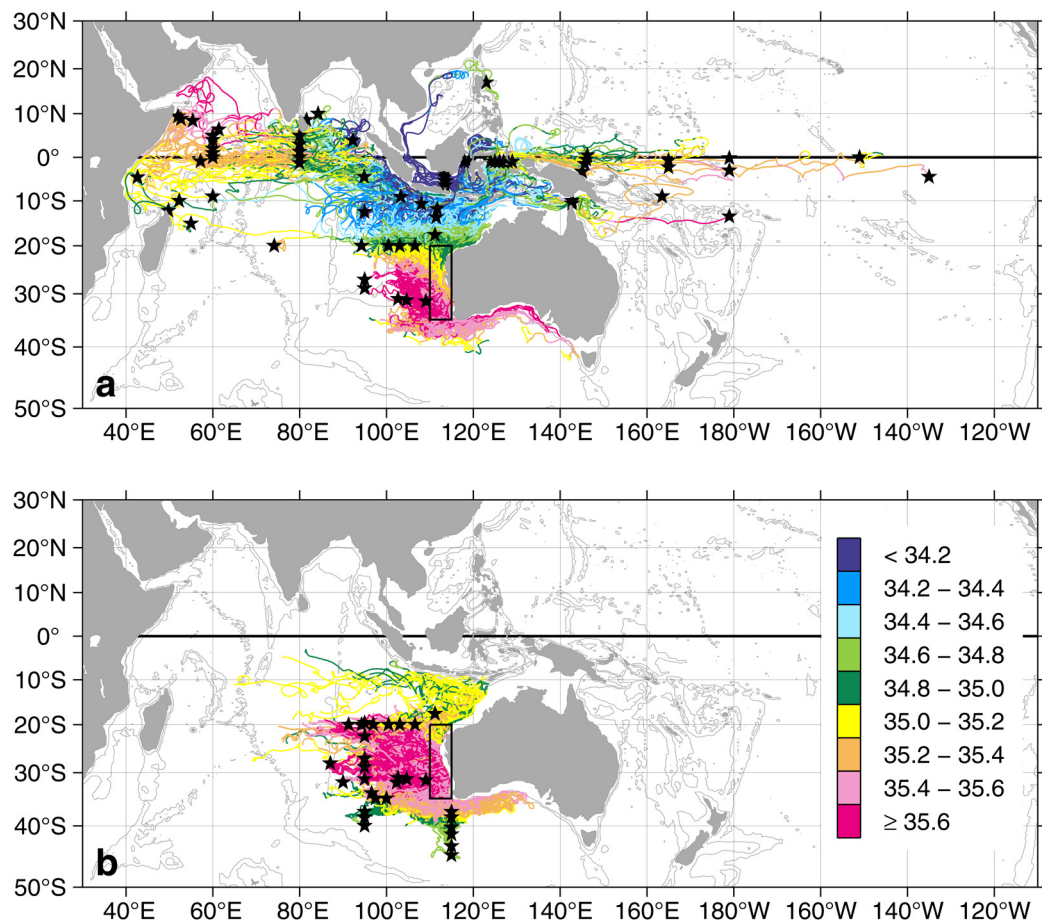| Group | Eastern Gyral | Subtropical Indian | South Indian |
|---|---|---|---|
| 25 m | - - - | - - - | - - - |
| 75 m | 35 | 162 | 16 |
| 150 m | 9 | 69 | 22 |
| 300 m | ∅ | 18 | 49 |
| 600 m | 7 | 9 | 33 |
| Sum | 51 | 258 | 120 |
| Total | 51 + 258 + 120 = **429** | | |

- - -  No Coverage

**Figure 4.2.** Numerical particle trajectories traversing the selected area (rectangle) off Western Australia from start points at depths ≤600 m. Trajectories associated with the Leeuwin Current (panel a). Trajectories associated with the Leeuwin Undercurrent and Subtropical Gyre (panel b). Colour represents salinity variation. Isobaths are 1000 and 3000 m (gray lines).
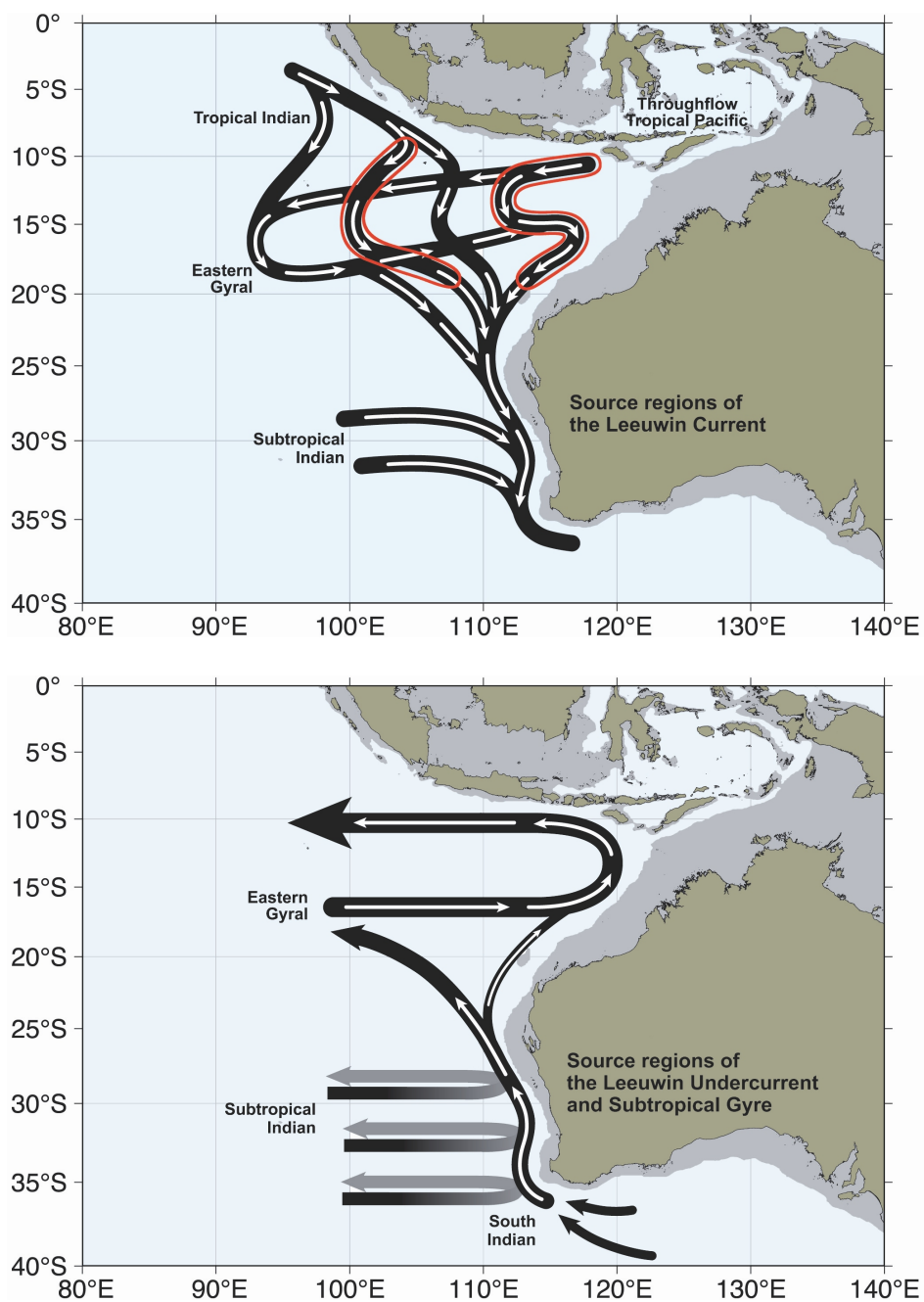
**Figure 4.3.** Schematic diagram of the circulation based on the numerical particle trajectories in **Figure 4.2**. Top panel: source regions of the Leeuwin Current. The "C" and "S" (via southern part of the North West Shelf) routes are exemplified by the red highlight (see text for details). Bottom panel: source regions of the Leeuwin Undercurrent. The alongstream deepening of the zonal jets in the Subtropical Indian (eastward near surface jets and deeper westward jets) are represented by the black to gray shading of the arrows.

### 4.3.1  Leeuwin Current

The water that flows in the Leeuwin Current [**Figure 4.4**] contains a tropical component advected from the Indo–Australian Basin [panels a, b, c] and a subtropical inflow from the Subtropical Gyre [panel d]. Associated salinities reveal the transition from fresh tropical waters to highly saline subtropical waters.

#### 4.3.1.1 Tropical source

Water particles come from the tropical Pacific Ocean via the Indonesian Throughflow or the tropical Indian Ocean via the South Java Current and follow two routes in the Indo–Australian Basin (top 100 m) before joining the Leeuwin Current. One of the routes depicts an "S" [**Figure 4.4**, panels a1, b1, c1] and the other a "C" [panels a2, b2, c2]. Both involve a near surface westward flow along the South Equatorial Current reversing into the Eastern Gyral Current. The difference among the routes lies in whether the particles transported by the Eastern Gyral Current are diverted directly into the Leeuwin Current near or south of 22°S ("C") or into a poleward boundary flow along the southern part of the North West Shelf ("S") that eventually augments the Leeuwin Current. Note that, the trajectories in panel d have start points along the domain of the Eastern Gyral Current that were not split into "S" or "C" routes, as this has been already made clear in other panels.

It has been long implied that the tropical source of the Leeuwin Current stems from an outflow from Timor Strait into the North West Shelf [e.g., Nof *et al.*, 2002] but this is not evident as a major pathway in **Figure 4.4**. Not many particles are seen to leave the Indonesian Seas via Timor Strait because Ombai Strait accommodates the bulk of the outflow by being artificially too wide in the model configuration (small islands not resolved), as formerly inferred in Gordon and McClean [1999]. While some of the past studies have suggested that the Leeuwin Current begins along the North West Shelf, others only recognise it as the poleward flow past North West Cape (22°S). Even though the trajectories reveal a poleward surface flow along the southern part of the North West Shelf, which augments the Leeuwin Current along the west Australian coast, we prefer to consider them two separate systems. The current along the continental slope of the North West Shelf is only poleward from April to August, as verified in the model Eulerian diagnostics (not shown) and in agreement with seasonal reversals observed in drifter measurements [Cresswell *et al.*, 1993]. Along the west Australian coast, the Leeuwin Current is a permanent year–round poleward flow [see **Chapter 5**].

A new aspect of the tropical source of the Leeuwin Current revealed by the particle trajectories, not seen elsewhere, is the link with the upper portion of the South Java Current [**Figure 4.4**, panels c1, c2] and other monsoonal currents in the tropical Indian [**Figure 4.1**, panel a]. The South Java Current is a semi–annually reversing jet

along the Java/Sumatra coasts with a maximum eastward flow during the monsoon transitions in May and November [Quadfasel and Cresswell, 1992; Meyers *et al.*, 1995]. Before reaching the South Java Current, particles travelling from the western and central tropical Indian Ocean may spend several months in large recirculation cells near the equator produced by frequent reversals of the monsoonal jets [Haines *et al.*, 1999; Schott *et al.*, 2002]. Although the trajectories shown in this study can only be understood in qualitative terms, an inclination for the particles from the tropical Indian to follow the "C" (28) rather than the "S" (10) route is apparent [**Table 4.1**]. This may cause an impact on the water properties of the Leeuwin Current along the west Australian coast. In addition, the particles from the "C" route which are not trapped along the boundary (near or south of 22°S and generally north of 25°S) join the Leeuwin Current with a Tropical Water that is more modified towards subtropical characteristics [e.g., **Figure 4.4**, panels a2,c2].

We suspect the near surface circulation depicted by the trajectories in the upper 100 m of the Indo–Australian Basin is shaped by a combination of Ekman and geostrophic flows at seasonal time scales. This seasonal variability may explain why particles from the tropical Indian apparently prefer the "C" route; why some of the particles flow along the North West Shelf and others do not; and also how the particles go across the swift westward regime of the South Equatorial Current to recirculate in the Eastern Gyral Current. For instance, southward Ekman transport is highly favoured in winter months [e.g., see wind stress pattern in **Figure 2.2** in **Chapter 2**].

### 4.3.1.2 Subtropical source

The subtropical inflow of the Leeuwin Current is represented by 13 trajectories from 5 start points, situated south of North West Cape (22°S) and at 75 m, that depict eastward flows before reaching the Australian coast [**Figure 4.4**, panel e]. Most of the start points lie near 30°S and their overall trajectories form a cyclonic gyre, composed by the eastward jets, the poleward Leeuwin Current and then westward offshoots. Andrews [1977] was the first to describe a cyclonic stream in the southeastern Indian Subtropical Gyre over the Naturaliste Plateau (29°–32°S) based on hydrographic observations, and in his terms, the summertime branch of the Western Australian Current. The Western Australian Current is deemed the equatorward branch of the wind–driven Subtropical Gyre [You and Tomczak, 1993; You, 1997] but earlier interpretations show no clear structure [Wooster and Reid, 1963] to no continuity of the equatorward flow [Wyrtki, 1962; Hamon, 1965]. Likewise the numerical trajectories do not provide any evidence of an equatorward Western Australian Current, at least in the upper ocean (0–300 m depth). The eastward jets which instead prevail owe their existence to the geostrophic adjustment that takes place in response to the large alongshore pressure gradient observed in the eastern Indian Ocean, which in turn, is transmitted from the western Pacific as a result of the communication between the two basins through the Indonesian Seas [Godfrey and Weaver, 1991].

### 4.3.1.3 Fate of the Leeuwin Current's waters

Once the tropical and subtropical inflows have joined the Leeuwin Current along the west Australian coast, they appear to have two primary fates [**Figure 4.4**]. One is westward advection to the ocean interior off Western Australia, including the region south of Cape Leeuwin (34°S), and the other is the boundary jet along the continental slope of the South Australian Basin, moving towards the west coast of Tasmania, in agreement with past observational evidences [e.g., Cresswell and Peterson, 1993; Ridgway and Condie, 2004]. The dominant path appears to be the offshore advection of particles into the Subtropical Gyre, most likely through the development of offshoots and shedding of mesoscale eddies. Mesoscale eddies are often observed to pinch off from wavelike protrusions of the Leeuwin Current between 20°S and 36°S [Griffiths and Pearce, 1985; Pearce and Griffiths, 1991]. Many of the numerical particles advected offshore, between the outer flank of the Leeuwin Current and east of 100°E, lie in an area populated by eddy motion [Morrow and Birol, 1998; Birol and Morrow, 2001]. These particles may be stalled there (or continue to move westward) for the rest of the model simulation or may return to the boundary, either within the Leeuwin Current or its undercurrent (sporadic).

Further insight into the fate of the Leeuwin Current particles in **Figure 4.4** can be better understood by examining cross–shelf distributions at three different latitudes, 22°S [**Figure 4.5**], 26°S [**Figure 4.6**] and 32°S [**Figure 4.7**]. The tropical Indian and Throughflow/Pacific sources of the Leeuwin Current (S and C routes) tend to fill the upper portion of the water column but may spread downwards where the current is deeper and less stratified at the coast. The Eastern Gyral and Subtropical Indian groups transport denser water, so their particles tend to fill the lower portion of the Leeuwin Current. Very few particles are seen to move into the Leeuwin Undercurrent (300–400 m). This just occurred for those which experienced considerable downwelling. The great majority of the particles reveal a strong lateral exchange between the boundary current and the ocean interior through zonal inflows and outflows. It is interestingly to note that, at least at 26°S, many of the numerical particles, for instance in the S route, that moved offshore (westward) are actually embedded in a mean eastward velocity field in the upper 200 m, implying that time variable flow is important.

The water mass transformations that accompany the trajectories along the west Australian coast are apparent in θ–S diagrams [**Figure 4.8**]. In essence, the Leeuwin Current begins as a very warm and relative fresh current at North West Cape (22°S) and by the time it reaches Cape Leeuwin (34°S) it has become saltier, cooler and denser. Part of this change in properties is caused by air–sea fluxes and part by exchange with the offshore ocean. The θ–S diagrams show that Tropical Water is converted into Subtropical Water (salinity maximum) and South Indian Central Water (below the salinity maximum), [e.g., panels b2, c2]. Subtropical Water is transformed into South Indian Central Water [panel e], though there is one example where it is actually transformed into warmer and fresher Tropical Water [**Figures 4.4 and 4.8**, panel e].
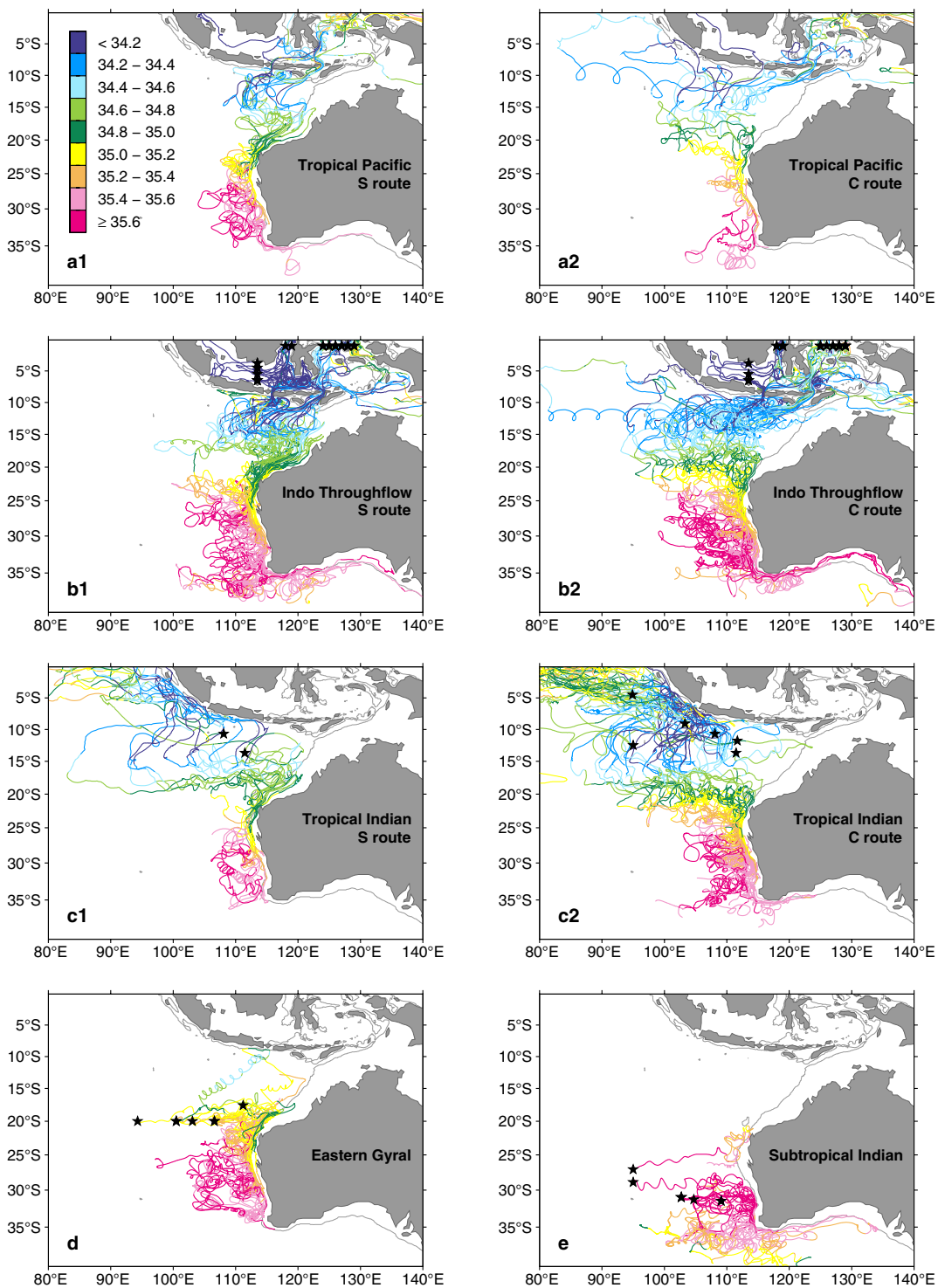
**Figure 4.4.** Numerical particle trajectories from tropical source regions of the Leeuwin Current [**Table 4.1**]. "S" route via North West Shelf. "C" route otherwise. Colour represents salinity variation. Isobath is 1000 m (gray line).
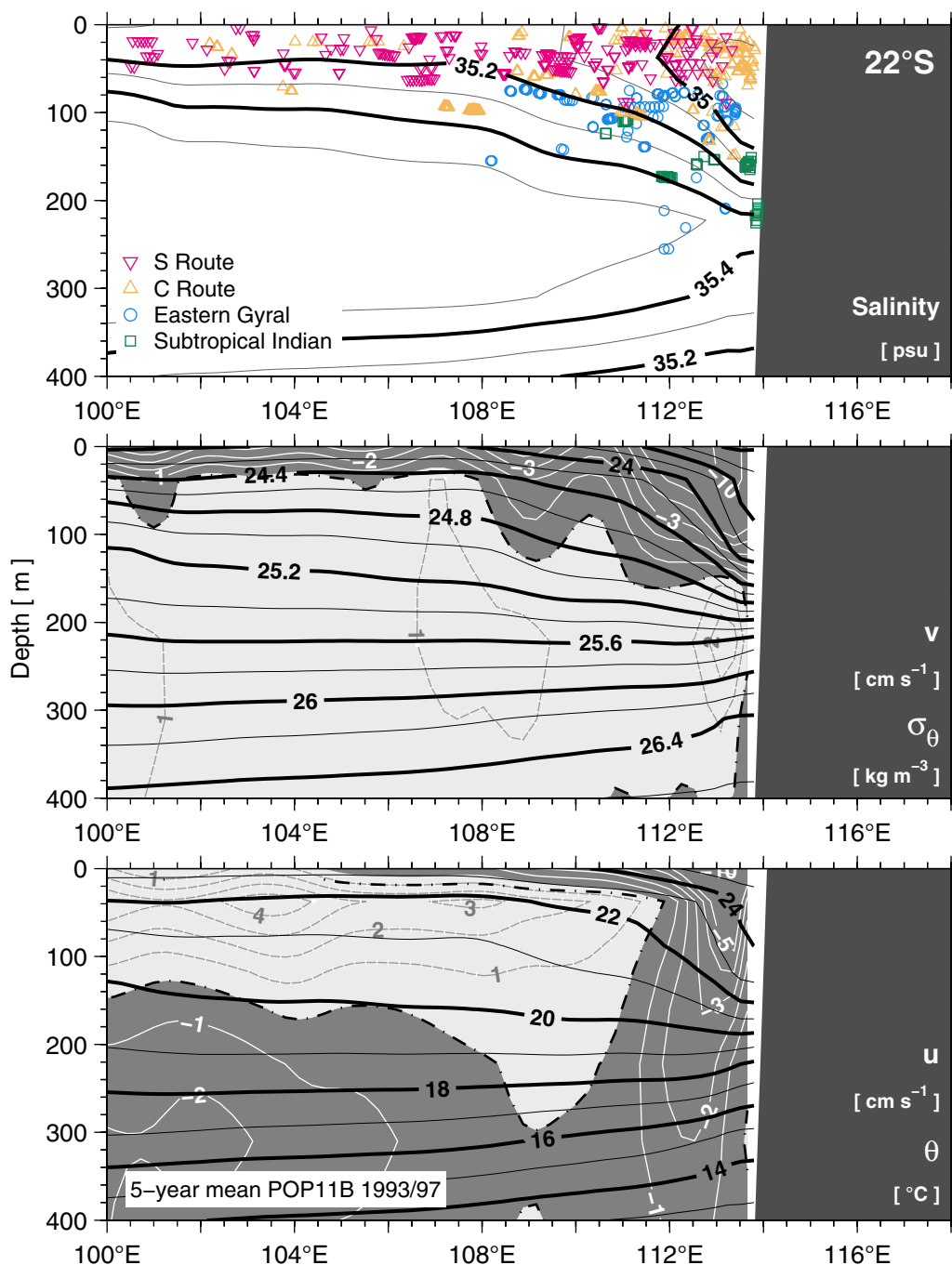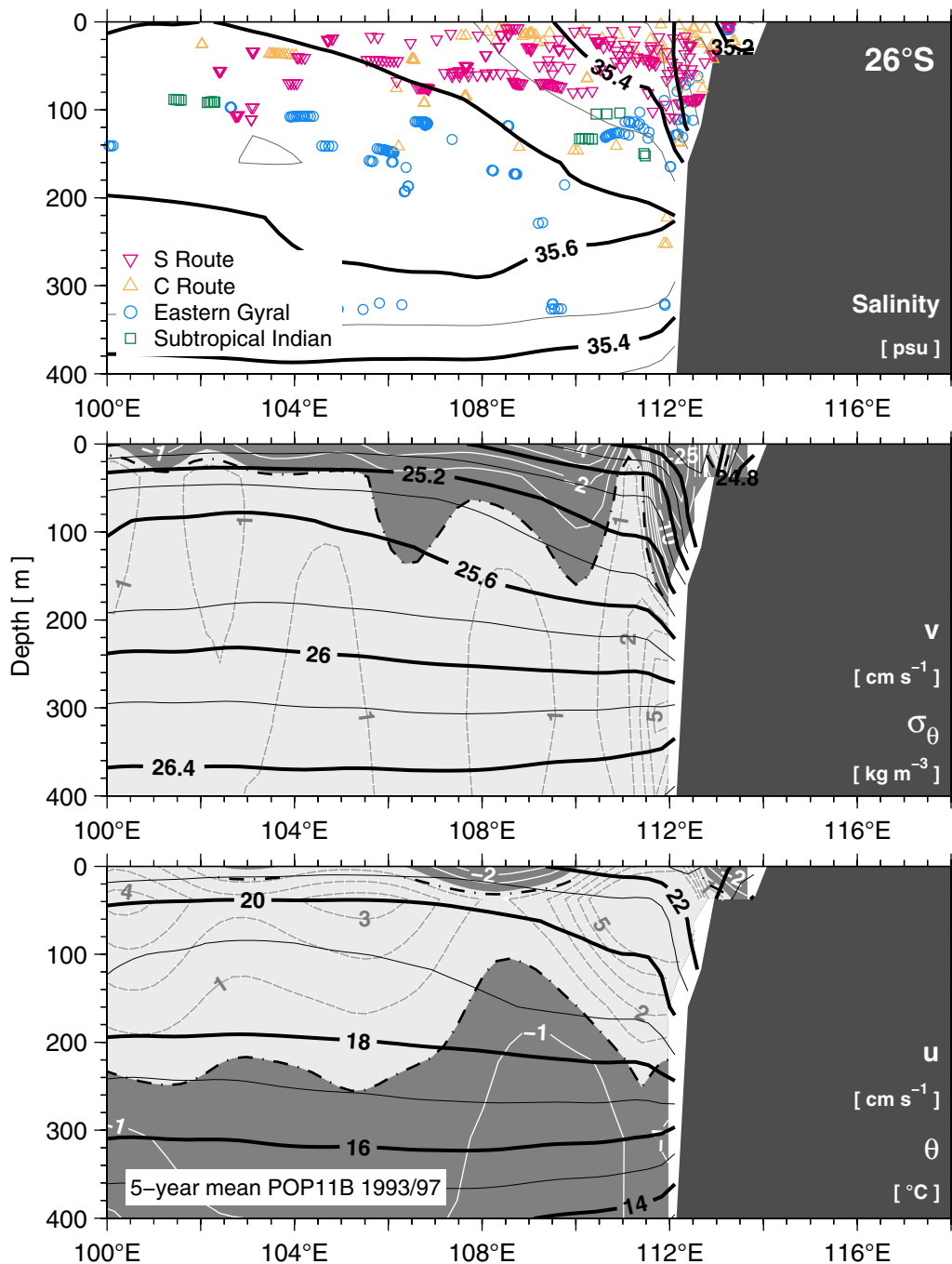
**Figure 4.5.** Cross–shelf section at 22°S (upper 400 m). Top panel indicates the depth distribution of the numerical trajectories associated with the Leeuwin Current [**Table 4.1**] on top of the salinity distribution. The middle panel is meridional velocity (+N) and $\sigma_\theta$ and the bottom panel is zonal velocity (+E) and $\theta$. All distributions are averaged for 1993/97.
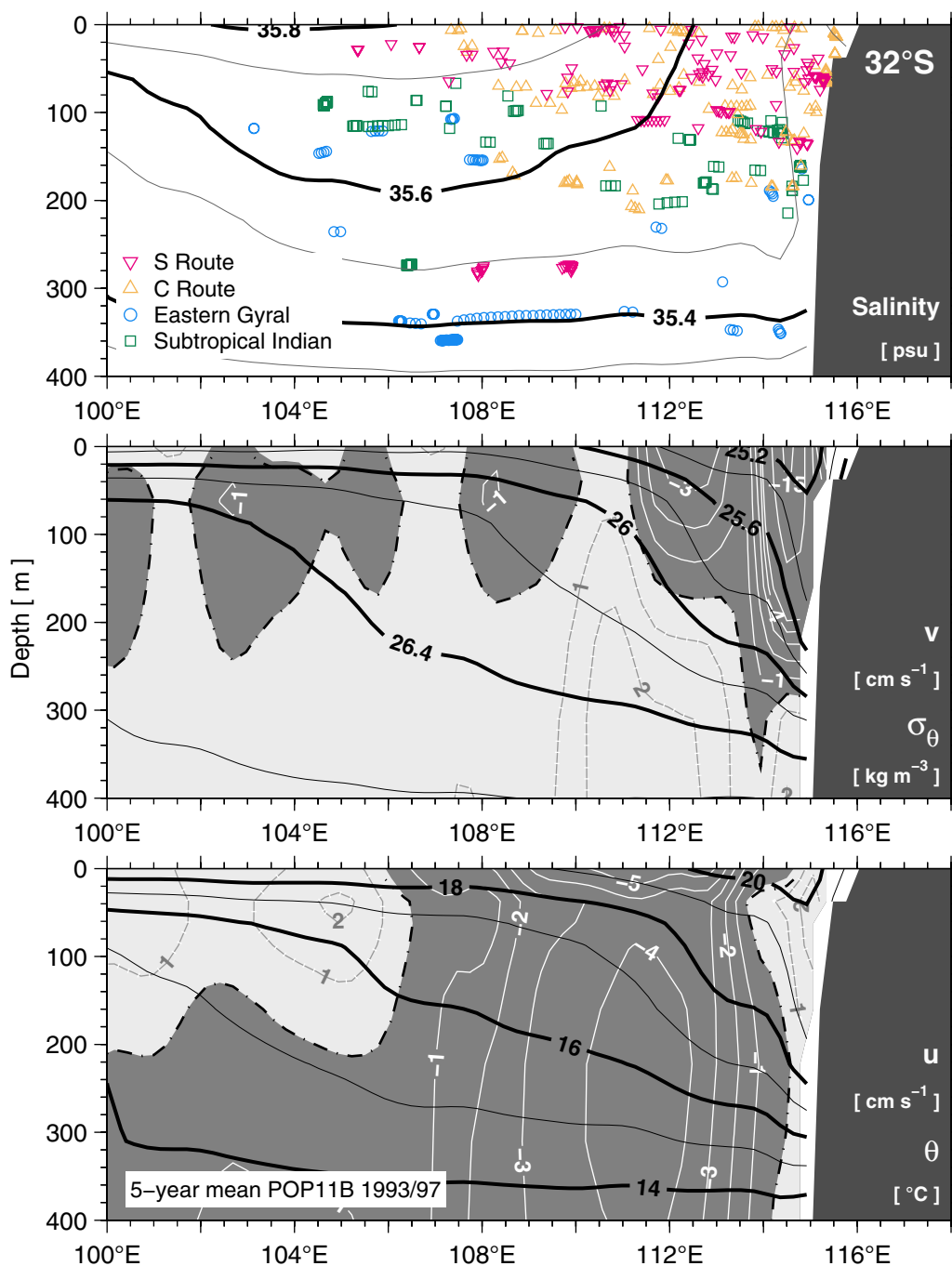
**Figure 4.6.** Cross–shelf section at 26°S (upper 400 m). Top panel indicates the depth distribution of the numerical trajectories associated with the Leeuwin Current [**Table 4.1**] on top of the salinity distribution. The middle panel is meridional velocity (+N) and $\sigma_\theta$ and the bottom panel is zonal velocity (+E) and $\theta$. All distributions are averaged for 1993/97.

**Figure 4.7.** Cross–shelf section at 32°S (upper 400 m). Top panel indicates the depth distribution of the numerical trajectories associated with the Leeuwin Current [**Table 4.1**] on top of the salinity distribution. The middle panel is meridional velocity (+N) and $\sigma_\theta$ and the bottom panel is zonal velocity (+E) and $\theta$. All distributions are averaged for 1993/97.
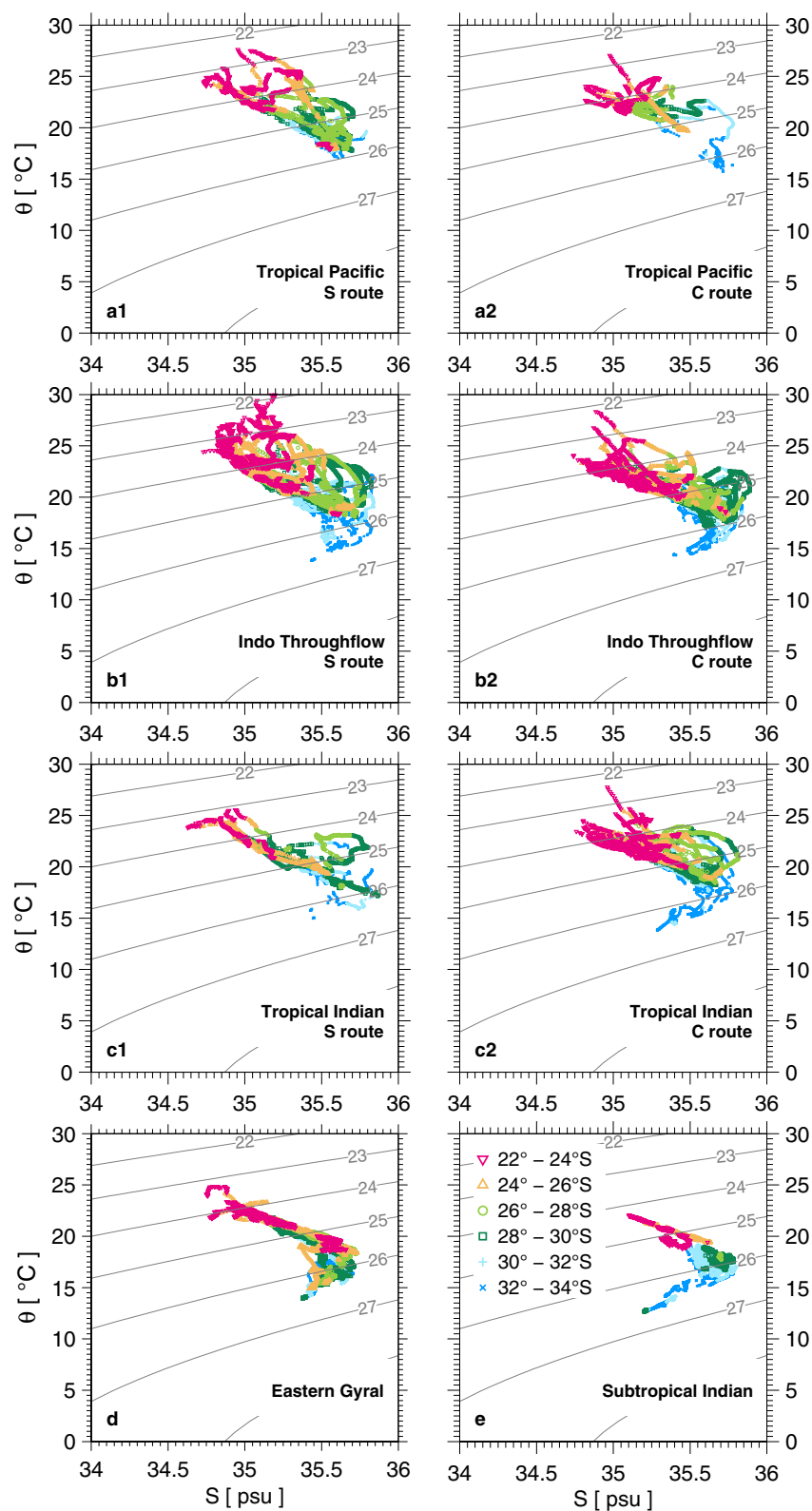
**Figure 4.8.** θ–S diagrams from source regions of the Leeuwin Current [**Table 1**]. Colour represents different latitude bands along the ocean off the west Australian coast.

### 4.3.2 Eastern Gyral Current

The Eastern Gyral Current was initially detected in XBT observations along the IX–1 line, running from Shark Bay/Australia (~25°S) to Sunda Strait/Indonesia (~7°S) [Meyers *et al.*, 1995; Wijffels *et al.*, 1996; Bray *et al.*, 1997]. It is a shallow current in the top 150–200 m flowing eastward along ~16°–20°S, immediately to the south of the swift and deep–reaching westward flow of the South Equatorial Current (~10°–15°S). The studies above have implied that the Eastern Gyral Current bifurcates near North West Cape (22°S), where one branch would continue towards the Indo–Australian Basin while the other would feed into the Leeuwin Current along the west Australian coast. Apparently the Eastern Gyral Current is driven by the same geostrophic adjustment that governs the subtropical eastward jets off Western Australia. The literature has always referred to it as a subtropical stream but we have verified in **Chapter 3** that its surface water is similar to the one advected poleward by the Leeuwin Current at 22°S, or in other words, both are of tropical origin (from north of 22°S). Presumably the Eastern Gyral Current has been always taken as a subtropical stream because its path lies closer to the subtropics, subject to more cooling and evaporation, and so its properties are not as warm and as fresh as those found in the South Equatorial Current.

The numerical trajectories herein not only confirm the hypothesis put forward by the studies cited above – that the Eastern Gyral Current is a shallow shear in the top 200 m which bifurcates near 22°S, with one branch feeding into the Leeuwin Current and the other flowing towards the Indo–Australian Basin – but actually gives a more detailed picture of the system. The upper part of the Eastern Gyral Current originates from southward flow across the South Equatorial Current, generally east of 80°E [**Figure 4.4**, panels a, b, c]. It is not clear, however, from where the deeper portion of the Eastern Gyral Current (start depths at 150 m) source its water from [**Figure 4.9**, panel a2]. In the 5–year mean zonal velocity section at 110°E, the Eastern Gyral Current is seen as two subsurface–intensified jets in the upper 200 m, one centred at 15°S and the other at 19°S [**Figure 4.11**]. The branch flowing to the Indo–Australian Basin has two fates. It indirectly augments the Leeuwin Current by veering into a surface poleward flow along the North West Shelf [**Figure 4.4**, panels a1, b1, c1, d] or it feeds into a subsurface equatorward flow along the North West Shelf [**Figures 4.9** and **4.11**]. This equatorward flow along the North West Shelf moves away from the boundary and ingress the westward South Equatorial Current, forming a large anticyclonic gyre (downward spiral) in the Indo–Australian Basin.
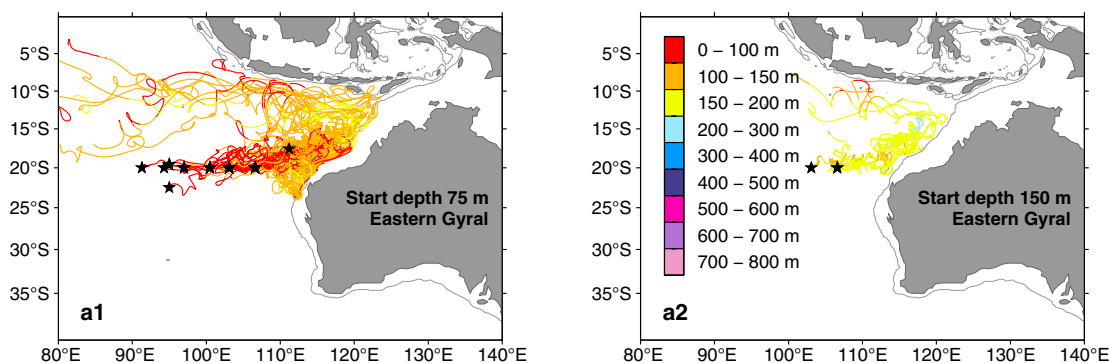
**Figure 4.9.** Numerical particle trajectories from the Eastern Gyral Current which are not a source for the Leeuwin Current [**Table 4.2**]. Colour represents depth variation. Isobath is 1000 m (gray line).

### 4.3.3  Leeuwin Undercurrent and Subtropical Gyre

We find a broad connection between the equatorward flow of the Leeuwin Undercurrent and the flows within the southeastern Indian Subtropical Gyre, as shown by the 429 trajectories in **Figure 4.10**. The total number of particles divided by group and start depth is listed in **Table 4.2**. The water masses involved in the pathways (not shown) are Subtropical Water (salinity maximum) and South Indian Central Water (linear θ–S relationship). The Leeuwin Undercurrent and the Subtropical Gyre are also known to advect Subantarctic Mode Water and Antarctic Intermediate Water (salinity minimum) but these water masses were not sampled by the trajectories used in this study [**Figure 4.11**].

The upper ocean circulation in the southeastern Indian is depicted by a large anticyclonic gyre [**Figure 4.10**]. Near surface eastward jets approach the west Australian coast to feed into the equatorward Leeuwin Undercurrent [panels a1, a2]. The Leeuwin Undercurrent, in turn, returns most of this inflow to the Subtropical Gyre as a series of deeper westward outflows [see **Figure 4.11**]. Only a smaller part continues north of 20°S, along the continental slope of the North West Shelf [**Figure 4.10**, panel a1], and we prefer not to deem this equatorward flow as part of the Leeuwin Undercurrent. The Eulerian diagnostics show that the variability of the currents along the North West Shelf are somewhat different from what is observed along the west Australian coast (not shown). The westward jets off Western Australia are also reinforced by outflows from the South Australian Basin [panels b1 to b4]. These outflows, before reaching the Leeuwin Undercurrent or the Subtropical Gyre, if in the upper 300–400 m, are often trapped in a small anticyclonic recirculation, presumably associated with the mesoscale activity commonly seen in satellite imagery near Cape Leeuwin (34°S) [e.g., Cresswell and Peterson, 1993].

The negative wind stress curl over the Subtropical Gyre drives an Ekman convergence and thus subduction of water parcels [Karstensen and Quadfasel, 2002a; Karstensen and Quadfasel, 2002b]. This is noticed, for instance, by the gradual deepening along the course of the eastward jets indicated by the change in colour [**Figure 4.10**, panel a1]. The downwelling in the ocean interior is very gradual, varying from several months to years. Near the west Australian coast, however, particles are likely to experience an abrupt downwelling, varying from some days to few months, usually accompanied by strong horizontal velocity shear. Immediately thereafter these particles are mostly found either in the Leeuwin Undercurrent or westward jets, as observed in the time series of some of the trajectories (not shown). The mechanisms that may explain this sudden downwelling are presumably associated with eddy induced subduction and also a more intense steepening of the thermocline slope near the coast, caused by the poleward flow of the Leeuwin Current [**Figures 4.5** to **4.7**].

Although past theoretical and modelling studies have implied that a broad geostrophic subtropical flow – which is in fact the succession of subsurface–intensified eastward jets within the Subtropical Gyre [**Figure 4.11**] – flows onshore to augment the Leeuwin Current [Thompson, 1987; Batteen and Rutherford, 1990], none of them have implied that it could also be a source for the Leeuwin Undercurrent. In **Chapter 3**, this link was implied by observing Subtropical Water at undercurrent's depths across a section at 22°S. In this chapter, the link has been confirmed by numerical particle trajectories. These same trajectories clarify another point of the regional circulation. By pinpointing that the salinity tongue is in effect formed by a combination of the zonal jets, onshore at surface and offshore at subsurface, embedded in a weaker background northerly drift [**Figure 4.11**] in addition to water exchange with the equatorward flow of the Leeuwin Undercurrent along the continental slope [**Figure 4.10**], they substitute the belief in which the tongue was simply proposed to result from subduction of Subtropical Water within the equatorward flow of the Western Australian Current along the eastern limb of the Subtropical Gyre [e.g., Toole and Warren, 1993; You and Tomczak, 1993]. Apparently, unless the Western Australian Current is regarded as the net effect of those flow patterns (anticyclonic gyre) or the meridional component of the zonal jets (weak northerly drift), it is not really an obvious feature. The northerly drift may result from Sverdrup dynamics whereas the zonal flows arise from the anomalously large alongshore pressure gradient in the eastern Indian Ocean. At surface this gradient would drive the eastward jets and its reversed gradient at depth would drive the westward jets [Thompson, 1984, 1987; Godfrey and Ridgway, 1985].
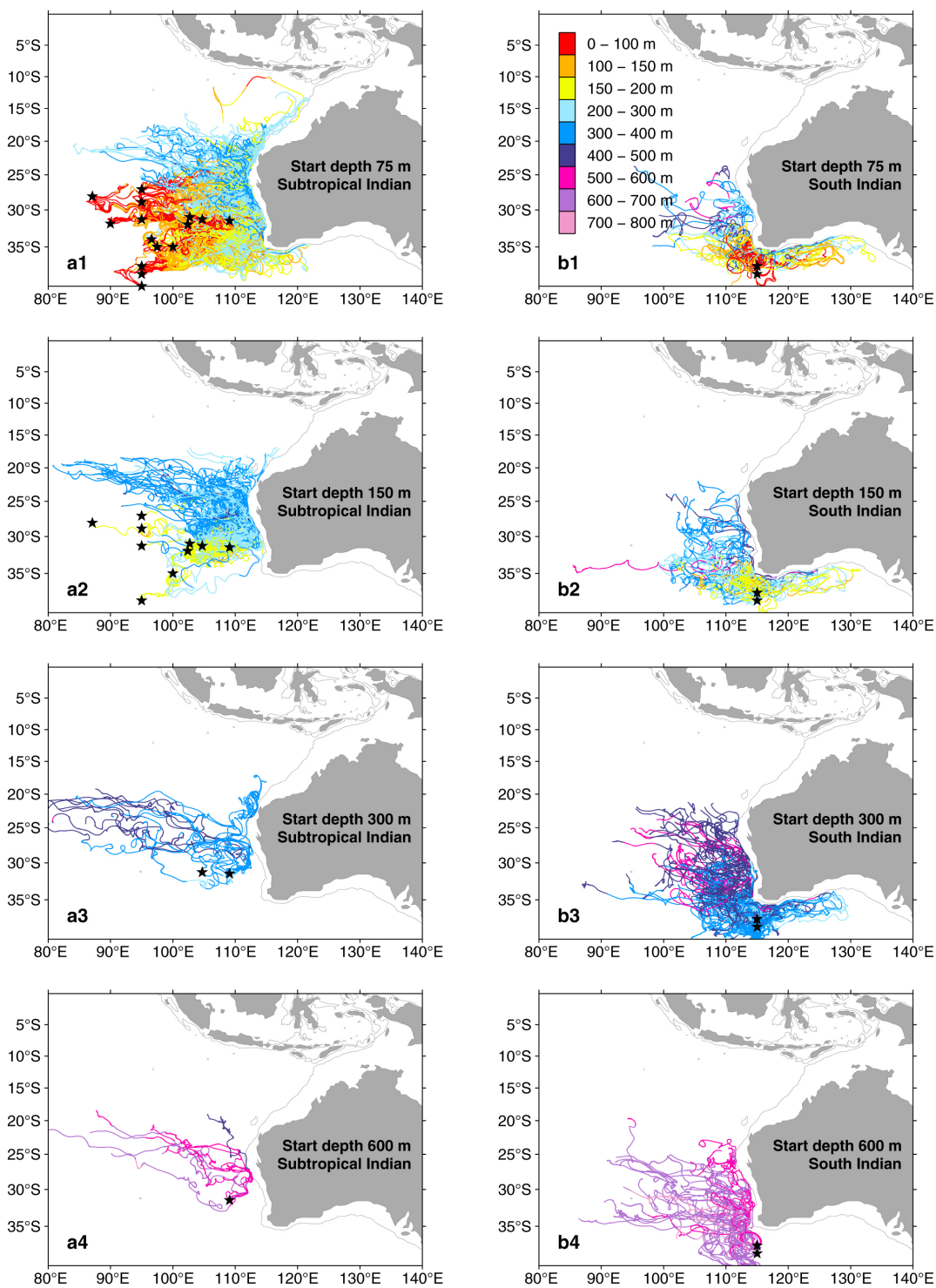
**Figure 4.10.** Numerical particle trajectories from source regions of the Leeuwin Undercurrent and Subtropical Gyre [**Table 4.2**]. Colour represents depth variation. Isobath is 1000 m (gray line).
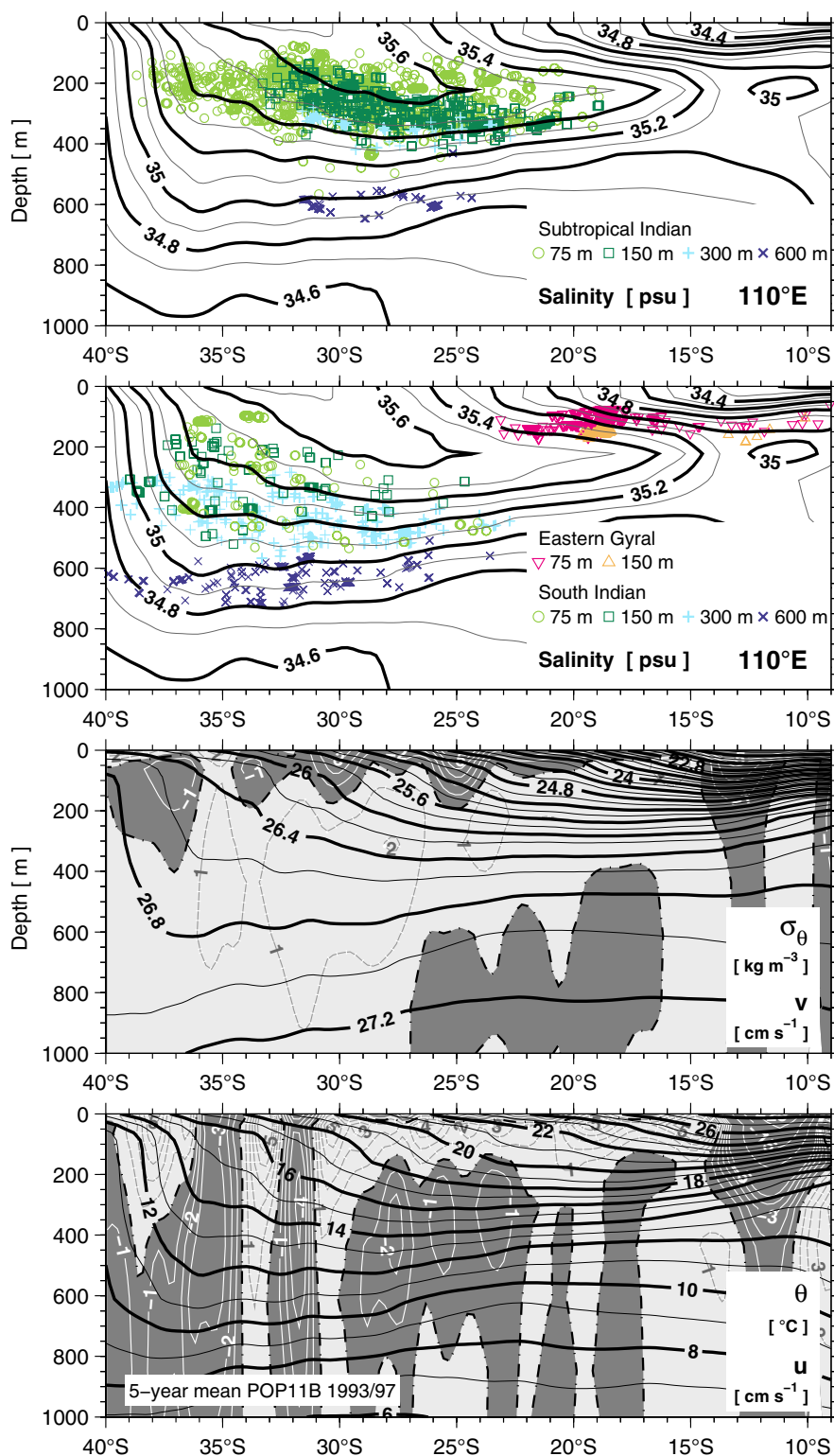
**Figure 4.11.** Along–shore section at 110°E (upper 1000 m). Top two panels indicate the depth distribution of the numerical trajectories listed in **Table 4.2** on top of salinity distribution. The middle panel is meridional velocity (+N) and $\sigma_\theta$ and the bottom panel is zonal velocity (+E) and $\theta$. All distributions are averaged for 1993/97.

## 4.4   CONCLUSIONS

Despite the qualitative nature of this study, the online particle tracking provides new insights on the links of the regional upper ocean circulation off Western Australia with the Leeuwin Current and the Leeuwin Undercurrent. In this Lagrangian perspective, the eastern boundary of the South Indian Ocean emerges as a "leaky" boundary. Extensive water exchange occurs between the boundary currents and the ocean interior (Subtropical Gyre) by means of a series of onshore and offshore jets. The results in general reveal that:

- The tropical source of the Leeuwin Current from the Indo–Australian Basin is not only of Pacific/Indonesian Throughflow origin but also of tropical Indian origin. The South Java Current (South Equatorial Current) operates as the conduit between the tropical Indian (tropical Pacific/Indonesian Throughflow) and the Indo–Australian Basin. Water property anomalies from these two different source regions are then likely transmitted to the west Australian coast by the Leeuwin Current.

- To reach the Leeuwin Current, Tropical Water does not necessarily come from a poleward surface boundary flow along the North West Shelf (the "S" route). Another pathway is identified as the "C" route. Both involve a southward traverse in the upper 100 m of the South Equatorial Current (~10°–15°S) and the Eastern Gyral Current (~16°–20°S). There is not a direct outflow from Timor Strait into the poleward surface flow along the North West Shelf. Whether this happens in the real ocean or is a model limitation is not yet clear though.

- The fact that there are two main routes in the Indo–Australian Basin before particles reach the Leeuwin Current may be important for the distribution of water properties, nutrients and planktonic organisms along the west Australian coast. Particles from the tropical Indian appear to have an inclination for the "C" route. Particles from the "S" route" may experience strong vertical mixing due to internal tides over the North West Shelf.

- The Eastern Gyral Current emerges as two subsurface–intensified jets instead of one. Its upper portion is fed by a recirculation of the South Equatorial Current, but it still is unclear how its lower portion is augmented. It can advect water back to the South Equatorial Current through a subsurface equatorward flow along the continental slope of the North West Shelf. However, at the same time, it can also feed the Leeuwin Current either through a surface poleward flow along the North West Shelf or a direct diversion of its eastward flow near North West Cape (22°S).

- The broad geostrophic inflow, thought as the subtropical source of the Leeuwin Current, is in effect a series of subsurface–intensified eastward jets. What has not been anticipated before is that they are a major source for the Leeuwin Undercurrent.

- Downwelling is broadly observed in the Subtropical Gyre. In the ocean interior, it appears gradual and mainly due to Ekman pumping. Near the west Australian coast, the particles flowing with the eastward jets can experience a relatively rapid downwelling, varying from some days to a few months, that basically contributes to the augmentation of the Leeuwin Undercurrent. Mesoscale eddies most possibly play a role in these sudden and irreversible vertical displacements of the particles. Another factor is the steep sloping of the isopycnals near the boundary associated with the Leeuwin Current.

- The simplistic view about the formation of the high salinity tongue of the Subtropical Gyre (subduction and equatorward movement by the West Australian Current) is substituted by a more complex explanation that basically involves a combination of near surface onshore flow and deeper offshore flow, both linked with the Leeuwin Undercurrent. The Western Australian Current appears only well defined if it is thought as the net displacement arising from the connectivity of those currents (an anticyclonic gyre) or alternatively the weak northerly drift in which the zonal jets are embedded.

- In addition to outflow from the Leeuwin Undercurrent, the deeper westward jets in the Subtropical Gyre are fed by northwestward flows from the southern Indian Ocean, inclusive from the South Australian Basin.

The POP11B online particle tracking has addressed many aspects of the upper ocean circulation of the southeastern Indian that were not well resolved in the literature but it has also contributed to a new perspective of the system. Even though it is important to remember that these results do not represent the complete circulation pattern of the southeast Indian Ocean. The trajectories shown herein are biased by the geographical location and depth of the start points, the 5–year duration of the POP11B simulation and selection criteria.

In the next chapter, we provide a quantitative picture of the mean and seasonal cycle of the current structure, the volume transport and the water properties of the Leeuwin Current along the west Australian coast (22°–34°S), using the model Eulerian diagnostics.